

# A general strategy for metallic nanocrystals synthesis in organic medium†

Peng Huang,<sup>a</sup> Jing Lin,<sup>b</sup> Zhiming Li,<sup>a</sup> Hengyao Hu,<sup>a</sup> Kan Wang,<sup>a</sup> Guo Gao,<sup>a</sup> Rong He<sup>a</sup> and Daxiang Cui<sup>\*a</sup>

Received 10th March 2010, Accepted 4th May 2010

First published as an Advance Article on the web 25th May 2010

DOI: 10.1039/c0cc00307g

**Herein we report a general synthesis strategy for metallic nanocrystals in a two-phase liquid–liquid system, which involves a quite fast nucleation stage overlapped with the growth stage within 10 min.**

The development of efficient methods for the controlled synthesis of nanocrystals with monodispersity, stability, and predictable morphology is one of the key goals in the advancement of nanoscience and nanotechnology.<sup>1</sup> Over the past 20 years, great efforts have been devoted to the development of various synthesis methods for preparing monodisperse nanocrystals. Recently, a two-phase approach has become a promising technique to challenge this key scientific problem.<sup>2</sup> Compared with other methods,<sup>3</sup> it has the following advantages: (1) Reaction of molecular precursors were spatially separated in the organic and aqueous phases; (2) The nucleation stage of nanocrystals overlapped with the growth stage only occurring at the liquid–liquid interface; (3) Product prepared in organic media can be easily self-assembled into close-packed hexagonal monolayers on solvent evaporation for various applications. To date, the two-phase approach has been exploited for the synthesis of a series of metallic, alloy, semiconductor and semiconductor–metal hybrid nanoparticles.<sup>2,4</sup> However, in the case of synthesizing metallic nanocrystals, the two-phase approach is not quite successful.<sup>5</sup> Further developments of the two-phase synthesis for metallic nanocrystals are desirable.

Metal nanoparticles such as silver and copper have attracted much attention because of their unique physical and chemical properties, and their tremendous applications in the area of catalysis, optical, magnetic, thermal, electronic devices, sensoric devices and SERS (surface enhanced Raman scattering).<sup>6</sup> Such properties and applications strongly depend on their size, size distribution and morphologies. However, the design and synthesis of nanostructured materials with controlled properties remain a significant challenge. Herein we report a general

protocol for transferring metal ions from water to an organic medium, which involves mixing a two-phase system containing metal salts with an aqueous solution of sodium oleate (SO), and then extracting the metal ions into an organic layer (toluene, hexane or other non-polar solvents). It was successfully applied towards the synthesis of a variety of metallic nanocrystals. Compared with other general approaches, this protocol allowed nanocrystals to be synthesized in an organic medium using aqueous soluble metal salts as starting materials, which are relatively inexpensive and easily obtained. It was easily extended to synthesize a large scale of nanomaterials for industrial production and application.

Our strategy is based on a general phase transfer and separation mechanism occurring at the interfaces of liquid–liquid systems without the separation of nucleation and growth processes, as shown in ESI Scheme 1.† The whole reaction goes on at room temperature and only needs about ten minutes. The concrete synthesis process consists of two steps: the first step is that sodium oleate is added into a vigorously stirring two-phase system with metal cations in the aqueous layer, two immiscible phases in the presence of the surfactant reverse micelles are formed, which needs about 3 min, as soon as the color of the aqueous phase becomes weak, the metal cations are quantitatively removed from this phase. The second step is the reduction of metal cations within reverse micelles by adding hydrazine hydrate (N<sub>2</sub>H<sub>4</sub>·H<sub>2</sub>O). The source of the electron, N<sub>2</sub>H<sub>5</sub><sup>+</sup>, is also captured by free surfactant molecules that are floating at the interface. The reduction of metal cations starts at the aqueous cores of reverse micelles, as a result of thermal Brownian motion. This step takes about 5 min to ensure that the reduction reaction is completely finished.

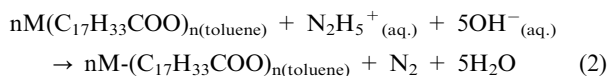
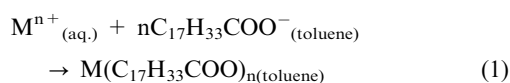
Sodium oleate plays many important roles throughout this process. It is firstly used as a phase-transfer agent, the Ag<sup>+</sup>, Cu<sup>2+</sup>, Ni<sup>2+</sup>, Co<sup>2+</sup>, Fe<sup>3+</sup>, or Fe<sup>2+</sup> ions in aqueous solution are firstly extracted into toluene. Then, the extracted metal ions are reduced into a critical composition of atomic species by rapidly adding hydrazine hydrate. Because metal atoms have a high surface activity, the extractant SO also acts as a capping agent to modify the surface of newly generated particles and to coordinate their carboxyl end groups, the hydrophobic carbon tails of the sodium oleate were pointed outwards from the surface of the synthesized particles. In addition, SO acts as a surfactant to form fluctuating structures that were postulated to behave as reactors or templates during synthesis. Meanwhile, charged surfactants often form complexes with the metal salt precursors, which may affect

<sup>a</sup> Department of Bio-Nano Science and Engineering, Key Laboratory for Thin Film and Microfabrication Technology of Ministry of Education, National Key Laboratory of Micro/Nano Fabrication Technology, Research Institute of Micro/Nano Science and Technology, Shanghai Jiao Tong University, Shanghai 200240, China. E-mail: dxcui@sjtu.edu.cn

<sup>b</sup> College of Chemistry, Chemical Engineering and Biotechnology, Donghua University, Shanghai 201620, China

† Electronic supplementary information (ESI) available: Experimental details, characterization and part results and discussions. See DOI: 10.1039/c0cc00307g

reduction kinetics. SO's function in this process was generally proposed on the basis of the following reactions.



A variety of metallic nanocrystals were obtained in a liquid–liquid system at room temperature. Typical reaction nodes were recorded by a camera shown in Fig. 1. From a to d, they respectively corresponded to Ag, Cu, Ni and Fe. The whole reaction was intentionally recorded into three nodes. Before adding the surfactant, the systems display two layers clearly. The lower color layer is the water phase containing metal ion and the upper colorless layer is the toluene phase. After adding the surfactant, the whole system turns into a consistent color without distinct layers. After the reducing agent was added, the system comes back to two layers. The lower layer turns clear and the upper layer contains a color, different from the former color of the metal ions. Fig. 1e–f show transmission electron microscope (TEM) images of typical samples of Ag, Cu, Ni, and Fe nanocrystals and indicates the large quantity and small size (<10 nm). The Ag nanocrystals are usually in round shapes with smooth surfaces, and self-assemble into ordered two-dimensional (2D) arrays on the surface of the TEM grid (Fig. 1e).

As shown in Fig. 1e–f, the metallic nanocrystals are approximately spherical with an average diameter of  $6.2 \pm 1.6$ ,  $3.2 \pm 0.6$ ,  $4.4 \pm 0.8$  and  $2.5 \pm 0.5$  nm, estimated by measuring 200 randomly selected particles in enlarged TEM images, corresponding to Ag, Cu, Ni and Fe, respectively. Thorough high resolution (HR) TEM characterizations revealed the highly crystalline nature of Ag and Cu nanocrystals (see supplementary data Fig. 1 and 2†). The histograms of Ag and Cu nanocrystals show the particle size distribution fitted by a Gaussian curve (see supplementary data Fig. 3 and 4†), but they are quite broad, which are identical with the references.<sup>5</sup> Therefore, the quality of obtained metallic nanocrystals should be substantially improved.

Based on Ostwald ripening (also referred to as coarsening) theory,<sup>7</sup> smaller particles are essentially consumed by larger particles during the growth process. Post-treatment at a high temperature to control size and promote crystallization is

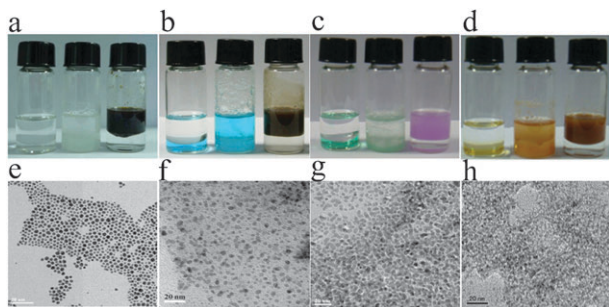


**Fig. 1** Photographs showing typical reaction nodes in toluene–water system (a:Ag; b:Cu; c:Ni; d:Fe) and TEM images of metallic nanocrystals (e:Ag; f:Cu; g:Ni; h:Fe)

necessary. Further studies on the quality of obtained metallic nanocrystals were implemented. The temperature of the ripening reaction was determined at  $\sim 150$  °C, only contraposing the organic phase (including the formed product) with using an autoclave, the time of extraction is adjustable for accurately controlling the size of the as-prepared nanocrystals.

TEM images of Ag nanocrystals after heat treatment for 2 h are shown in Fig. 2a and b, which indicates the Ag nanoparticles are spherical with a narrow size distribution ( $\sim 6.5$  nm). Compared with Fig. 1e, the tiny nanoparticles disappeared and are consumed by larger particles during the growth process. The inset is the corresponding SAED pattern in an area including many Ag nanocrystals, revealing that the nanocrystals are polycrystalline. The observed diffraction rings can be indexed as (111), (200), (220) and (311) reflections, respectively. Fig. 2c shows the UV-vis absorption spectra of Ag nanocrystals before (1) and after heat treatment (2) in the 300–700 nm wavelength range, using toluene as the solvent. Curve (1) has a special absorption peak at 412 nm. Curve (2) exhibits no obvious shift of absorption peak position and significant enhancement of absorption at 412 nm. The absorption intensity and half-peak width are both correlated to the particle size of the nanomaterials. According to this principle, we can conclude that the size of the latter is bigger than the former, which is consistent with TEM image results. Fig. 2d is the XRD pattern of Ag nanocrystals after heat treatment. The characteristic (111), (200), (220) and (311) peaks could be indexed as the face-centered cubic silver, which are in agreement with the standard card (JCPDS: 04–0783).

TEM images of Cu nanocrystals after heat treatment for 10 h are shown in Fig. 3a and b, which indicate the Cu nanoparticles are spherical with a narrow size distribution ( $\sim 10$  nm). Compared with Fig. 1f, the tiny nanoparticles disappeared and are consumed by larger particles during the growth process. The inset is the corresponding SAED pattern in an area including many Cu nanocrystals, revealing that the

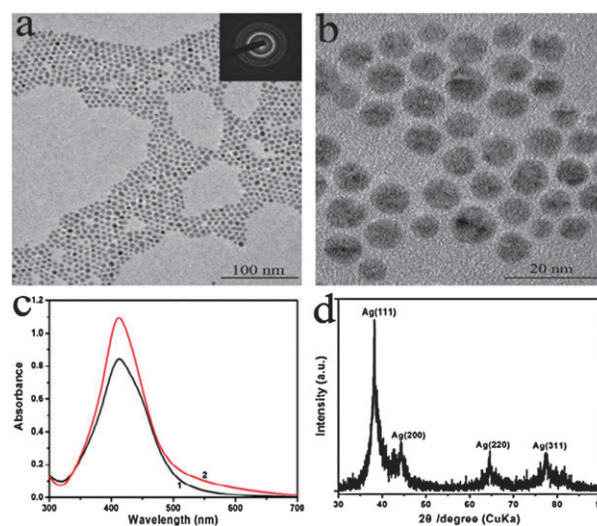


**Fig. 2** (a) Low magnification TEM image of Ag nanocrystals after heat treatment and corresponding electron diffraction pattern (inset). (b) High magnification TEM image, (c) UV-vis spectra of Ag nanocrystals before (1) and after heat treatment (2), and (d) XRD pattern of Ag nanocrystals after heat treatment.

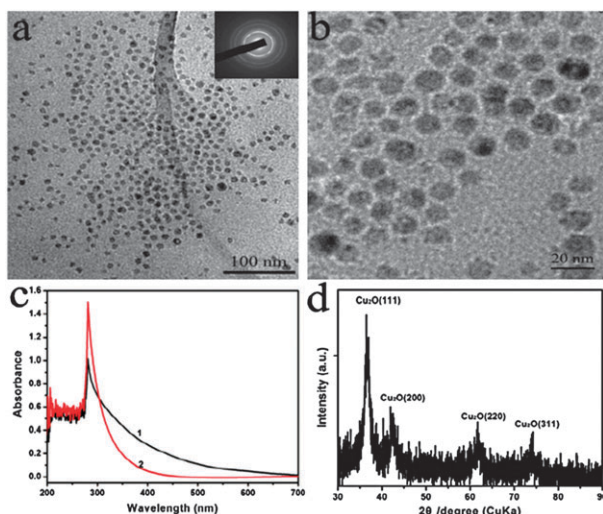


**Fig. 3** (a) Low magnification TEM image of Cu nanocrystals after heat treatment and corresponding electron diffraction pattern (inset). (b) High magnification TEM image, (c) UV-vis spectra of before (1) and after heat treatment (2), and (d) XRD pattern of Cu nanocrystals after heat treatment.

nanocrystals are polycrystalline. Fig. 3c shows the UV-vis absorption spectra of Cu nanocrystals before (1) and after heat treatment (2) in the 200–700 nm wavelength range. Curve (1) has a special absorption peak at 280 nm. Curve (2) exhibits no obvious shift of absorption peak position and significant enhancement of absorption at 280 nm. Fig. 3d is the XRD pattern of Cu nanocrystals after heat treatment, the characteristic (111), (200), (220) and (311) peaks are typical of  $\text{Cu}_2\text{O}$  crystallinity.

In addition, we also used the above-mentioned method to synthesize large scale nanoparticles such as Ag, Cu, Ni, Fe and Co nanoparticles with the amounts of 5 g with a yield of > 95% (see supplementary data Fig. 5 and 6†). Based on the synthesis of metallic nanocrystals, we also successfully prepared alloy, semiconducting, and magnetic nanocrystals in supplementary data Fig. 7.†

In summary, we established a simple, general, and controlled approach to synthesize large-scale monodisperse metallic nanocrystals with a narrow size distribution such as Ag, Cu, Ni, Fe and Co nanoparticles. A possible mechanism for the formation of monodisperse nanocrystal is also discussed in the supplementary information.†<sup>8–21</sup> This method can be further broadened to prepare various nanomaterials, including alloy, magnetic, semiconductive, and rare-earth fluorescent

nanocrystals. Our results lay the foundation for industrial production and application of the metal nanoparticles.

This work is supported by China National 973 Project (No. 2010CB933901), National 863 Hi-tech Project (2007AA0-22004), National Natural Scientific Fund (No. 20771075 and No. 20803040), New Century Excellent Talent of Ministry of Education of China (NCET-08-0350), Shanghai Science and Technology Fund (No. 10XD1406100 and No. 072112006-6).

## Notes and references

- (a) Y. Zhu and Y. Qian, *Sci. China, Ser. G*, 2009, **52**, 13; (b) J. Park, J. Joo, S. Kwon, Y. Jang and T. Hyeon, *Angew. Chem., Int. Ed.*, 2007, **46**, 4630; (c) D. Wang, W. Zheng, C. Hao, Q. Peng and Y. Li, *Chem. Commun.*, 2008, 2556.
- (a) D. Pan, Q. Wang and L. An, *J. Mater. Chem.*, 2009, **19**, 1063; (b) J. Yang and J. Ying, *Nat. Mater.*, 2009, **8**, 683.
- (a) B. Cushing, V. Kolesnichenko and C. O'Connor, *Chem. Rev.*, 2004, **104**, 3893; (b) X. Wang, J. Zhuang, Q. Peng and Y. Li, *Nature*, 2005, **437**, 121.
- D. Pan, X. Ji, L. An and Y. Lu, *Chem. Mater.*, 2008, **20**, 3560.
- (a) N. Peng, *J. Am. Chem. Soc.*, 2003, **125**, 47; (b) N. Zheng, J. Fan and G. Stucky, *J. Am. Chem. Soc.*, 2006, **128**, 6550.
- (a) Y. He-long, X. Yi, S. Pei-jing, X. Bin-shi, W. Xiao-li and L. Qian, *Trans. Nonferrous Met. Soc. China*, 2008, **18**, 636; (b) C. Rao and A. Cheetham, *J. Mater. Chem.*, 2001, **11**, 2887; (c) Y. Sun and Y. Xia, *Science*, 2002, **298**, 2176.
- (a) P. Voorhees, *J. Stat. Phys.*, 1985, **38**, 231; (b) G. Oskam, Z. Hu, R. Penn, N. Pesika and P. Searson, *Phys. Rev. E: Stat., Nonlinear, Soft Matter Phys.*, 2002, **66**, 11403.
- M. Faraday, *Philos. Trans. R. Soc. London*, 1857, **147**, 145.
- M. Brust, M. Walker, D. Bethell, D. Schiffrin and R. Whyman, *J. Chem. Soc., Chem. Commun.*, 1994, 801.
- (a) A. Kasuya, R. Sivamohan, Y. Barnakov, I. Dmitruk, T. Nirasawa, V. Romanyuk, V. Kumar, S. Mamykin, K. Tohji and B. Jeyadevan, *Nat. Mater.*, 2004, **3**, 99; (b) N. Zhao, D. Pan, W. Nie and X. Ji, *J. Am. Chem. Soc.*, 2006, **128**, 10118.
- Q. Yu, C. Liu, Z. Zhang and Y. Liu, *J. Phys. Chem. C*, 2008, **112**, 2266.
- A. Swami, A. Kumar, M. D'Costa, R. Pasricha and M. Sastry, *J. Mater. Chem.*, 2004, **14**, 2696.
- D. Jian and Q. Gao, *Chem. Eng. J.*, 2006, **121**, 9.
- J. Wan, X. Chen, Z. Wang, W. Yu and Y. Qian, *Mater. Chem. Phys.*, 2004, **88**, 217.
- D. Leff, L. Brandt and J. Heath, *Langmuir*, 1996, **12**, 4723.
- S. Horswell, C. Kiely, I. O'Neil and D. Schiffrin, *J. Am. Chem. Soc.*, 1999, **121**, 5573.
- W. Liu, X. Wang and S. Fu, in *Process for producing copper nanoparticles*, Google Patents, 2004.
- D. Pan, S. Jiang, L. An and B. Jiang, *Adv. Mater.*, 2004, **16**, 982.
- S. Chen, K. Huang and J. Stearns, *Chem. Mater.*, 2000, **12**, 540.
- (a) M. Kovalenko, M. Bodnarchuk, R. Lechner, G. Hesser, F. Schaffler and W. Heiss, *J. Am. Chem. Soc.*, 2007, **129**, 6352; (b) N. Wu, L. Fu, M. Su, M. Aslam, K. Wong and V. Dravid, *Nano Lett.*, 2004, **4**, 383.
- (a) V. LaMer and R. Dinegar, *J. Am. Chem. Soc.*, 1950, **72**, 4847; (b) J. Park, V. Privman and E. Matijevic, *J. Phys. Chem. B*, 2001, **105**, 11630.